NeuroImage 55 (2011) 1454–1460

Contents lists available at ScienceDirect

NeuroImage

journal homepage: www.elsevier.com/locate/ynimg

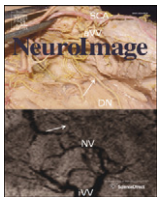

Radial diffusivity predicts demyelination in *ex vivo* multiple sclerosis spinal cords ☆,☆☆

Eric C. Klawiter [a,*], Robert E. Schmidt [b], Kathryn Trinkaus [c], Hsiao-Fang Liang [d], Matthew D. Budde [d], Robert T. Naismith [a], Sheng-Kwei Song [d], Anne H. Cross [a], Tammie L. Benzinger [d]

[a] Department of Neurology, Washington University School of Medicine, 660 South Euclid Avenue, Campus Box 8111, Saint Louis, MO 63110, USA
[b] Department of Pathology and Immunology, Washington University School of Medicine, 660 South Euclid Avenue, Campus Box 8118, St. Louis, MO 63110, USA
[c] Division of Biostatistics, Washington University School of Medicine, 660 South Euclid Avenue, Campus Box 8067, St. Louis, MO 63110, USA
[d] Department of Radiology, Biomedical MR Laboratory, Washington University School of Medicine, Campus Box 8227, 660 South Euclid Avenue, St. Louis, MO 63110, USA

ARTICLE INFO

Article history:
Received 12 July 2010
Revised 24 November 2010
Accepted 5 January 2011
Available online 13 January 2011

Keywords:
Multiple sclerosis
Diffusion tensor imaging
Postmortum
Spinal cord

ABSTRACT

Objective: Correlation of diffusion tensor imaging (DTI) with histochemical staining for demyelination and axonal damage in multiple sclerosis (MS) *ex vivo* human cervical spinal cords.
Background: In MS, demyelination, axonal degeneration, and inflammation contribute to disease pathogenesis to variable degrees. Based upon *in vivo* animal studies with acute injury and histopathologic correlation, we hypothesized that DTI can differentiate between axonal and myelin pathologies within humans.
Methods: DTI was performed at 4.7 T on 9 MS and 5 normal control fixed cervical spinal cord blocks following autopsy. Sections were then stained for Luxol fast blue (LFB), Bielschowsky silver, and hematoxylin and eosin (H&E). Regions of interest (ROIs) were graded semi-quantitatively as normal myelination, mild (<50%) demyelination, or moderate–severe (>50%) demyelination. Corresponding axonal counts were manually determined on Bielschowsky silver. ROIs were mapped to co-registered DTI parameter slices. DTI parameters evaluated included standard quantitative assessments of apparent diffusion coefficient (ADC), relative anisotropy (RA), axial diffusivity and radial diffusivity. Statistical correlations were made between histochemical gradings and DTI parameters using linear mixed models.
Results: Within ROIs in MS subjects, increased radial diffusivity distinguished worsening severities of demyelination. Relative anisotropy was decreased in the setting of moderate–severe demyelination compared to normal areas and areas of mild demyelination. Radial diffusivity, ADC, and RA became increasingly altered within quartiles of worsening axonal counts. Axial diffusivity did not correlate with axonal density ($p = 0.091$).
Conclusions: Increased radial diffusivity can serve as a surrogate for demyelination. However, radial diffusivity was also altered with axon injury, suggesting that this measure is not pathologically specific within chronic human MS tissue. We propose that radial diffusivity can serve as a marker of overall tissue integrity within chronic MS lesions. This study provides pathologic foundation for on-going *in vivo* DTI studies in MS.
© 2011 Elsevier Inc. All rights reserved.

Introduction

Multiple sclerosis (MS) is an inflammatory disease of the central nervous system (CNS) that commonly results in disability (Noseworthy et al., 2000). Spinal cord involvement is common in MS, even early in disease (Bot et al., 2004a). Multiple sclerosis plaques contain marked pathologic heterogeneity, with variable demyelination, axonal damage, gliosis, remyelination and inflammation (Barnes et al., 1991). While demyelination may be considered the hallmark of MS pathology, axonal damage is hypothesized to be the histologic substrate for disability (Trapp et al., 1998). Axonal loss can occur early in active disease (Ferguson et al., 1997; Ghosh et al., 2004) and is commonly observed later in the disease subtypes of primary progressive MS (PPMS) and secondary progressive MS (SPMS) (Tallantyre et al., 2009).

Brain magnetic resonance imaging (MRI) lesion load on T2 weighted (T2W) images correlates only modestly with physical disability in MS

Abbreviations: MS, multiple sclerosis; CNS, central nervous system; PPMS, primary progressive multiple sclerosis; SPMS, secondary progressive multiple sclerosis; MRI, magnetic resonance imaging; T2W, T2 weighted; DTI, diffusion tensor imaging; ADC, apparent diffusion coefficient; RA, relative anisotropy; ROI, region of interest; WMT, white matter tract; LFB, Luxol fast blue; H&E, hematoxylin and eosin; NAWM, normal-appearing white matter; ICC, intraclass correlation coefficient; ANOVA, one-way analysis of variance; SPSS, Statistical Package for the Social Sciences; FA, fractional anisotropy; DAWM, diffusely abnormal white matter.

☆ The corresponding author takes full responsibility for the data, the analyses and interpretation, and the conduct of the research. The corresponding author guarantees the accuracy of the references. The corresponding author has full access to all the data and has the right to publish any and all data, separate and apart from the attitudes of the sponsor.

☆☆ The Methods section includes a statement of compliance with institutional standards for the use of human subjects and tissue for this study.

* Corresponding author. Massachusetts General Hospital, 15 Parkman Street, WAC 835, Boston, MA 02446, USA. Fax: +1 617 726 6991.
E-mail address: eklawiter@partners.org (E.C. Klawiter).

1053-8119/$ – see front matter © 2011 Elsevier Inc. All rights reserved.
doi:10.1016/j.neuroimage.2011.01.007

(Barkhof, 1999; Brex et al., 2002). In addition, correlation of conventional spinal cord parameters with disability is weak at both 1.5 and 3.0 T MR field strengths (Nijeholt et al., 1998; Stankiewicz et al., 2009). While conventional MRI, including T2W, is relatively sensitive to spinal cord abnormalities, it lacks specificity to the underlying pathologic correlate. In addition, spinal cord axonal loss occurs largely independent of T2 changes (Bergers et al., 2002). Advanced imaging techniques to improve pathologic specificity and correlate with physical disability would be clinically valuable.

Diffusion tensor imaging (DTI) measures microscopic movement of water in tissues. Diffusion tensor imaging provides information on CNS tissue integrity and structure (Filippi et al., 2001). The directional diffusivity derived from DTI measurements describes microscopic water movement parallel to ($\lambda_{||}$, axial diffusivity) and perpendicular to ($\lambda_{\perp}$, radial diffusivity) axonal tracts. We have previously shown in mouse models of white matter injury that *decreased* $\lambda_{||}$ is associated with acute axonal injury, and *increased* $\lambda_{\perp}$ is associated with myelin injury (Budde et al., 2009; Song et al., 2002, 2003, 2005). Additionally, in a rat spinal cord model, DTI detects axonal damage distal to inflammatory lesions, perhaps secondary to Wallerian degeneration (DeBoy et al., 2007). In humans, $\lambda_{||}$ has been demonstrated to decrease with acute optic neuritis (Naismith et al., 2009). Also, $\lambda_{\perp}$ increases with clinical disability and severe tissue injury (Naismith et al., 2010a, 2010c).

This study sought to determine the relationship between DTI parameters and histopathology in human *ex vivo* spinal cord in the setting of chronic MS. The spinal cord provides an excellent model to study directional diffusion because axons within white matter tracts run in parallel, without significant crossing. As *in vivo* spinal cord DTI studies are explored (Agosta et al., 2007; Benedetti et al., 2010; van Hecke et al., 2009), it is important to understand the pathologic correlate of DTI parameters. A validated histopathology correlation study is a necessary prerequisite to the interpretation of *in vivo* spinal cord DTI studies. Our hypothesis was that $\lambda_{\perp}$ would differentiate among degrees of demyelination, whereas $\lambda_{||}$ would provide information about axonal damage.

Methods

Specimen preparation

Institutional standards were followed for the use of human subjects and tissue for this study. Cervical spinal cords were obtained following autopsy from 13 clinically definite MS subjects and eight normal control subjects. Four MS subjects and three controls were excluded due to T2* artifact on MRI. Cervical spinal cord blocks were fixed in 10% formalin in PBS at room temperature. Time from expiration to beginning fixation ranged from 4 to 16 h. Specimens remained in fixative for 7–10 days before being cut into blocks.

Magnetic resonance imaging

MRI was performed using an Oxford Instruments 200/330 magnet (4.7 T, 33-cm clear bore) equipped with a 15-cm inner diameter, actively shielded Oxford gradient coil (18 G/cm, 200-μs rise time). The magnet, gradient coil, and Techron gradient power supply were interfaced with a Varian UNITY-INOVA console controlled by a Sun Microsystems Ultra-60 Sparc workstation. A custom-made sample holder and a custom-made 8 mm solenoid surface coil were used for transmission and reception.

A conventional multislice spin echo imaging sequence modified by adding the Stejskal–Tanner diffusion sensitizing gradient pair was employed for acquisition of the required series of diffusion weighted images. The diffusion weighted images were acquired with repetition period (TR) 3 s, spin echo time (TE) 43 ms, time between application of gradient pulses 25 ms, diffusion gradient on time 10 m, slice thickness 0.25 mm with 0.25 mm isotropic voxels. Diffusion sensitizing gradients were applied along six directions with *b*-values of 0 and 1.813 ms/μm^2 (Basser and Pierpaoli, 1998). After imaging processing and averaging, the diffusion tensor was diagonalized to derive directional diffusivity on a voxel-by-voxel basis. Diffusion tensor imaging parameter maps were calculated for apparent diffusion coefficient (ADC), relative anisotropy (RA), $\lambda_{||}$, and $\lambda_{\perp}$ as previously described (Song et al., 2002). In addition, conventional T2W images were obtained at the same resolution.

ROI identification

A neuroradiologist (T.L.B.) blinded to pathologic and clinical data independently identified regions of interest (ROIs) within lesions from the T2W and DTI parameter maps. Additionally, standard ROIs were created for white matter tracts (WMTs) including the dorsal white matter, right and left lateral white matter, and right and left ventral WMTs (Fig. 1). These standard column ROIs were applied to all slices of control subjects to derive normal values for DTI parameters in human cervical spinal cords *ex vivo*.

Histological staining

Following DTI, the formalin fixed MS and control spinal cords were embedded in paraffin and cut on a sliding microtome at a thickness of 3 μm. Sections were stained with Luxol fast blue (LFB) for myelin quantification, Bielschowsky silver for axonal counts, and hematoxylin and eosin (H&E) for inflammatory infiltrates. Methods of grading myelin, counting axons and determining presence of inflammation were pre-determined by an experienced neuropathologist (R.E.S.). A single investigator (E.C.K.) blinded to MRI and clinical data independently identified ROIs from LFB stained sections using a Nikon 80i microscope (Nikon USA). Histologic white matter ROIs were identified and graded as: 1) normal myelination, 2) mild demyelination (>50% myelin staining preserved), or 3) moderate to severe demyelination (<50% myelin staining preserved) (Fig. 2) similar to previous grading systems (Bot et al., 2004b; Cook et al., 2004). An attempt to identify a group of regions characterized by severe demyelination (>90%) was made. However, the paucity of this observation in only a few samples precluded valid statistical analysis. Regions most representative of normal myelination in MS samples were selected to represent MRI-described normal-appearing white matter (NAWM). Myelin scoring was determined by one investigator (E.C.K.). A second investigator (T.L.B.) reviewed the myelin scores for each ROI and agreed with the first investigator's determination in all cases. Next, ROIs as identified by LFB staining were co-registered on immediately adjacent sections stained with Bielschowsky silver stain. Axons within ROIs were counted manually at magnified 40x high power fields. The H&E stained slides were evaluated for evidence of active inflammation, marked by inflammatory infiltrates. Specimens were graded as inflammation present or absent. Normal control

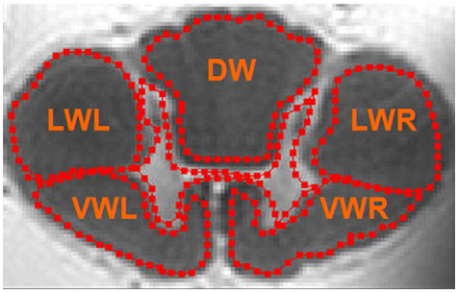

Fig. 1. White matter tract ROIs. Regions of interest are drawn to incorporate spinal cord white matter WMTs including dorsal white matter, left and right lateral white matter, and left and right ventral white matter WMTs.

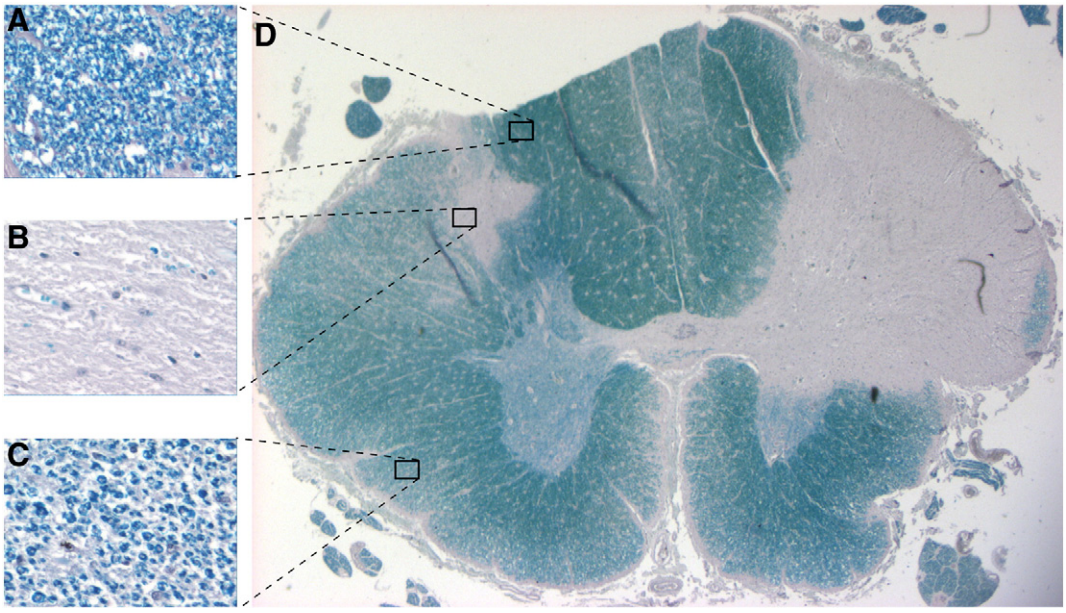

Fig. 2. Luxol fast blue myelin staining and scoring. An axial LFB staining of cervical spinal cord (panel D) exhibits variable degrees of demyelination in an MS subject. Panel A demonstrates relatively normal myelination. Panel B represents severe demyelination. Panel C represents mild demyelination.

sections were analyzed to confirm normal myelination and axonal density.

Pathologic and DTI co-registration

All image processing procedures were written in Java and implemented as plug-ins in ImageJ (NIH). Inter-modality registration of the spinal cord MR images was performed using a manual, 2D registration. Corresponding landmarks were manually placed on the DTI parameter maps and each of the digital histological images. Landmarks included vessels, prominent white and gray matter boundaries, and points along the perimeter of the cord. The co-registration of histological images to MR images was performed using a modification of previously described methods (Budde et al., 2007, 2009). Histologic images were warped to the pixelated MR image using a thin-plate spline warp deformation grid (Bookstein, 1989). Regions of interest identified on histologic sections were mapped on co-registered DTI slices (Fig. 3). Similarly, ROIs identified by DTI parameters were mapped on co-registered histologic sections. Values for each DTI parameter were determined for each ROI.

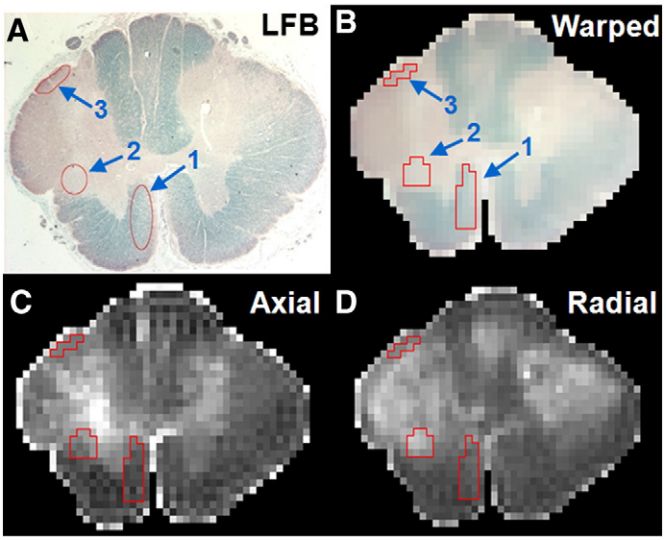

Fig. 3. Co-registration of histology to MRI images. A. A Luxol fast blue stained histologic slice is labeled with three ROIs (1–3). B. The histology image is warped with co-registered pixels to axial and radial diffusivity parameter maps (panels C and D).

Chart review

Autopsy reports and subject charts were reviewed following MRI and histology analysis to evaluate the subjects' demographics, clinical course and cause of death.

Statistical analysis

Inter-rater (E.C.K. and R.T.N.) axonal count reliability was assessed by intraclass correlation coefficient (ICC). Diffusion tensor imaging parameters and axonal count distributions were assessed and transformed as appropriate to approximate a Gaussian distribution to permit linear modeling. Mixed modeling compared DTI parameter means between control and MS subjects while accounting for multiple observations within a sample. Regional differences in MS spinal cords were analyzed by one-way analysis of variance (ANOVA). Linear mixed modeling with appropriate covariance structures were used to model DTI parameters by myelin and axonal pathologies. Multiple group comparisons were corrected using the Bonferroni correction. The distribution of axonal count as a continuous variable did not permit linear modeling due to poor model fit. As a result, this variable was analyzed in quartiles for correlation with DTI parameters. Possible pathology interactions were also assessed. Analysis was carried out using Statistical Package for the Social Sciences version 16 (SPSS, Chicago, IL).

Table 1
Demographics of MS subjects.

Subject #	Age	Race	Gender	Disease duration	Signs and symptoms potentially referable to the spinal cord	Disability level
1	48	AA	M	4	RLE weakness, spasticity	Walker
2	74	C	F	29	Tetraparesis	Wheelchair
3	59	C	M	14	Tetraparesis, diffuse paresthesias	Wheelchair
4	45	C	F	16	LLE weakness, BUE Numbness	N/A
5	45	C	F	17	Tetraplegia, incontinence	Wheelchair
6	88	C	M	57	Spastic tetraparesis, RUE numbness	Wheelchair
7	46	C	M	20	Tetraplegia, hyperreflexia	Wheelchair
8	54	C	F	22	Tetraparesis, Sensory level	Wheelchair
9	50	C	F	12	Spastic paraparesis	Wheelchair
Mean	56.6			21.2		

AA = African American; C = Caucasian; M = Male; F = Female; LLE = left lower extremity; BUE = bilateral upper extremities; RUE = right upper extremity; N/A = not available.

Results

Demographics

Mean age at expiration for MS subjects was 56.6 (±15.0) years (Table 1). Average disease duration was 21.2 (±15.1) years. All MS subjects had signs and symptoms referable to the spinal cord. Additionally, all MS subjects had significant physical disability prior to death. Cause of death in the majority of MS subjects was infectious. Mean age at expiration for control subjects was 47.8 (±20.1) years.

Tract analysis

Mean $\lambda_{||}$, $\lambda_{\perp}$, ADC and RA were derived from standard WMT ROIs as illustrated in Fig. 1. Twenty-five WMT ROIs from control subjects and 45 WMT ROIs from MS subjects, representing five standard WMT ROIs from a single slice in each subject, were averaged. Axial diffusivity, radial diffusivity and ADC were significantly higher for the MS WMT ROIs ($p<0.001$, respectively). In contrast, mean RA for the MS WMTs was not significantly different from controls ($p=0.54$) (Fig. 4). Among the MS subject ROIs, no differences for any of the DTI parameters were observed among the three WMT locations (dorsal, lateral, or ventral) by ANOVA ($\lambda_{||}$, $p=0.51$; $\lambda_{\perp}$, $p=0.60$; ADC, $p=0.47$; and RA, $p=0.74$). Time to fixation did not correlate with any of the DTI parameters ($\lambda_{||}$, $p=0.96$; $\lambda_{\perp}$, $p=0.31$; ADC, $p=0.55$; and RA, $p=0.25$). Mean WMT axonal density for control samples was 149 +/− 52 axons per high power field. Mean WMT axonal density for MS samples was 75 +/− 62 axons per high power field. Intraclass correlation coefficient of axonal determination was acceptable (ICC = 0.99).

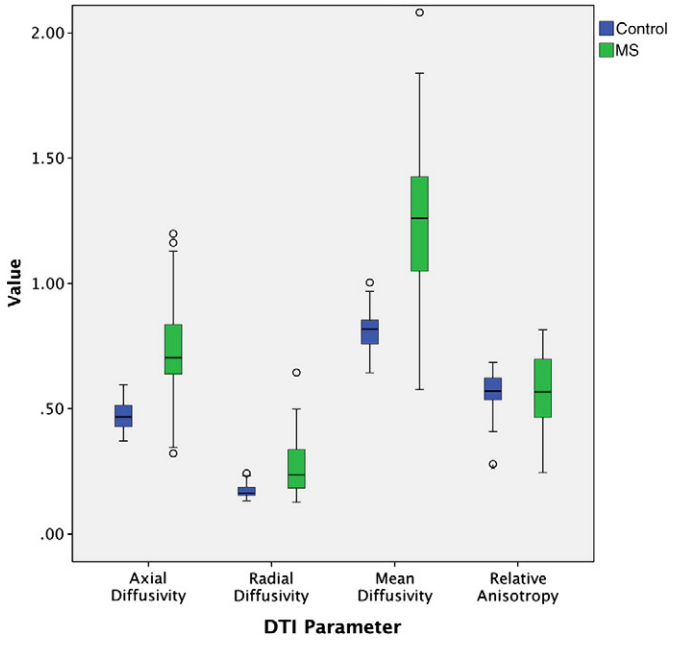

Fig. 4. DTI parameter means. Box plots of DTI parameters with boxes representing 25th–75th percentiles. Whiskers represent two standard deviations from the mean. Outliers are represented by circles and stars. Axial, radial, and mean diffusivity were each different between MS subjects and controls ($p<0.001$ for each) but no difference was appreciated for RA ($p=0.54$).

ROI analysis

Regions of interest were independently identified using the DTI parameter maps and histology. Diffusion values for each set of ROIs were not significantly different for any of the mean parameter values ($\lambda_{||}$, $p=0.67$; $\lambda_{\perp}$, $p=0.57$; ADC, $p=0.98$; and RA, $p=0.32$). As a result, comparison of DTI parameters to histologic markers was made as a combined group of ROIs derived from MRI and ROIs derived from histology.

Myelin analysis

Regions of interest were scored as control, normal myelination in MS spinal cords, mild demyelination or moderate to severe demyelination. Radial diffusivity increased as the degree of demyelination increased, and was the only parameter that differentiated among the three categories within MS spinal cords (Fig. 5). Also for $\lambda_{\perp}$, control ROIs were different from mild and moderate to severe MS regions, but not for areas of normal myelination in MS ($p=0.112$, pair-wise comparison) (Table 2). In addition to $\lambda_{\perp}$, $\lambda_{||}$and ADC both increased with increased degree of demyelination ($p<0.001$ each for linear trend). Relative anisotropy distinguished ROIs with moderate to severe demyelination from areas of normal myelin staining ($p<0.001$,

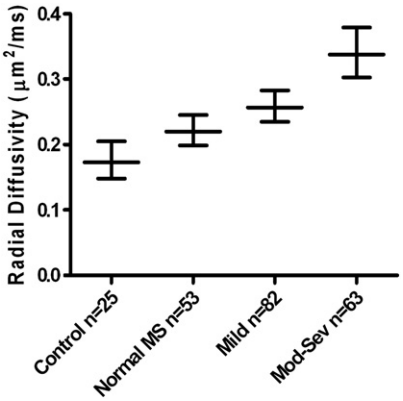

Fig. 5. Demyelination versus radial diffusivity. Radial diffusivity increases with increased degree of demyelination. Means are surrounded by 95% confidence intervals.

Table 2
Pair-wise comparisons of diffusion parameters at different levels of demyelination.

DTI parameter	Control: normal MS	Control: mild	Control: moderate/severe	Normal MS: mild	Normal MS: moderate/severe	Mild: moderate/severe
Radial diffusivity	0.173, 0.220; $p=0.112$	0.173, 0.257; $p=0.001$	0.173, 0.338; $p<0.001$	0.220, 0.257; $p=0.020$	0.220, 0.338; $p<0.001$	0.257; 0.338; $p<0.001$
Axial diffusivity	0.467, 0.675; $p=0.004$	0.467, 0.716; $p<0.001$	0.467, 0.824; $p<0.001$	0.675, 0.716; $p=0.578$	0.675, 0.824; $p<0.001$	0.716, 0.824; $p<0.001$
ADC	0.818, 1.159; $p=0.003$	0.818, 1.253; $p<0.001$	0.818, 1.552; $p<0.001$	1.159, 1.253; $p=0.299$	1.159, 1.552; $p<0.001$	1.253, 1.552; $p<0.001$
RA	0.553, 0.591; $p=1.000$	0.553, 0.548; $p=1.000$	0.553, 0.479; $p=0.972$	0.591, 0.548; $p=0.524$	0.591, 0.479; $p<0.001$	0.548, 0.479; $p=0.002$

Four groups of ROIs were compared including control ROIs, regions of normal myelination in MS spinal cords, mild demyelination and moderate to severe demyelination. The estimated marginal means for each diffusion tensor imaging parameter were compared between groups in a pair-wise fashion. A Bonferroni correction for multiple comparisons was applied to each *p*-value. Number of ROIs in each myelination category are: control 25, normal MS = 53, mild = 82, moderate to severe = 63 . Areas of normal myelination and mild demyelination were represented in all MS spinal cords. Moderate to severe regions were identified in 7 of 9 MS spinal cords.

pair-wise comparison) and mild demyelination (p=.002) (Fig. 6). Differences in $\lambda_{||}$ ($p=0.004$) and ADC ($p=0.003$), but not $\lambda_{\perp}$ ($p=0.112$) and RA ($p=1.000$), existed in pair-wise comparisons of controls and ROIs representative of NAWM in MS samples (Table 2).

Axonal and inflammation analyses

Axonal counts for each ROI were categorized into quartiles. Each DTI parameter was correlated with axonal density. Axial diffusivity did not predict axonal count density ($p=0.091$) (Fig. 7). Increased $\lambda_{\perp}$, increased ADC and decreased RA predicted a linear trend for axonal loss ($p<0.001$, $p=0.001$, and $p<0.001$, respectively). Only one of the nine MS subjects demonstrated inflammatory infiltrates on H&E staining.

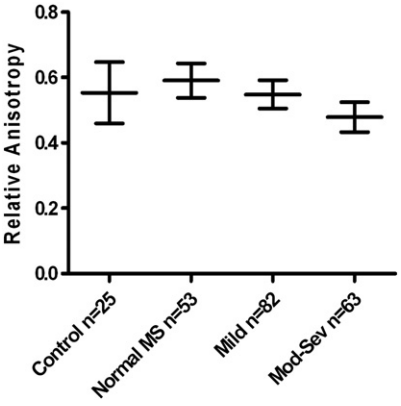

Fig. 6. Degree of demyelination versus relative anisotropy. Areas of moderate to severe demyelination demonstrate decreased relative anisotropy compared to controls but other categories are not statistically distinguishable. Means are surrounded by 95% confidence intervals.

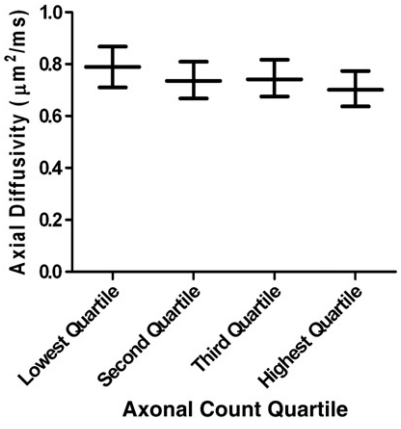

Fig. 7. Axonal density versus axial diffusivity. Poor correlation is demonstrated between the axonal count, separated by quartile, and axial diffusivity. The lowest quartile represents ROIs with the lowest axonal counts. The highest quartile represents ROIs with the highest axonal counts. Means are surrounded by 95% confidence intervals.

Combined pathology analysis

MS samples were analyzed for both myelin and axonal pathologies. All ROIs from the three myelin categories were then dichotomized into high or low axonal counts based upon the mean count for the MS ROIs. Thus, six histological categories included: 1) normal myelination with high axon count, 2) normal myelination, low axon count, 3) mild demyelination, high axon count, 4) mild demyelination, low axon count, 5) moderate to severe demyelination, high axon count, and 6) moderate to severe demyelination, low axon count. For each parameter, the interaction term between myelin and axonal pathologies was not significant indicating that DTI parameter differences did not vary between axonal groups differentially based on the degree of demyelination. A trend for increased $\lambda_{\perp}$ with increased demyelination and axonal loss was further delineated (Fig. 8).

When both myelin and axonal count were simultaneously analyzed as predictors of DTI parameters, there was evidence that both types of pathology contributed independently to changes in radial diffusivity (myelin $p<0.001$; axonal $p<0.001$, linear trends), RA (myelin $p=0.003$; axonal $p=0.001$), and mean diffusivity (myelin $p<0.001$; axonal $p=0.007$). However, when modeling axial diffusivity, only demyelination ($p<0.001$) was a significant predictor in the model, while axonal loss ($p=0.304$) was not.

A direct comparison of axonal counts and level of demyelination revealed a linear relationship ($p<0.001$) for decreased axonal counts with increased demyelination.

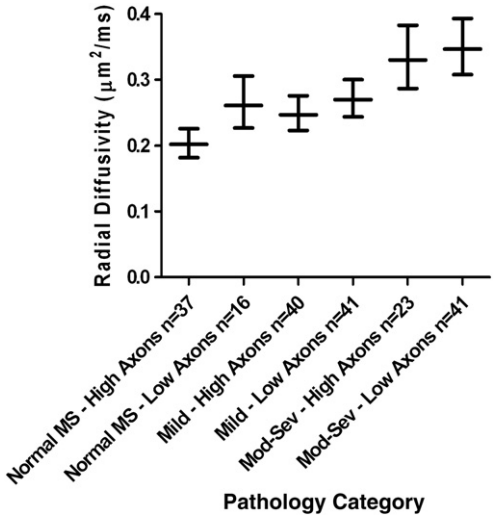

Fig. 8. Radial diffusivity by myelination and axonal density. Six groups of varying pathology demonstrate increase radial diffusivity with increase degree of demyelination and axonal loss. Means are surrounded by 95% confidence intervals.

Discussion

This histopathology correlation study examined DTI in the cervical spinal cord of MS subjects *ex vivo*. The parallel orientation of fibers in the spinal cord white matter tracts allowed for evaluation of directional diffusivity in addition to summary parameters such as ADC and RA. A striking finding of this study was the sensitivity of $\lambda_{\perp}$ to demyelination, supporting our original hypothesis. Radial diffusivity predicted level of demyelination, even when controlling for axonal loss in the statistical model. This finding corroborates previously published histopathology correlation studies in animal models (Song et al., 2002, 2003, 2005). While level of demyelination was also a significant predictor of axial diffusivity, radial diffusivity better distinguished regions with milder demyelination from the most normal areas in MS spinal cords. However, in the setting of chronic lesions, where normal tissue architecture is more significantly altered, radial diffusivity loses specificity for demyelination. Both level of demyelination and axonal density contributed to alterations in radial diffusivity, perhaps attributable to the correlation of the two types of pathology in these specimens with advanced damage. However, its associations with both demyelination and axonal damage suggest that radial diffusivity can serve as a marker of overall tissue integrity within chronic MS lesions.

Contrary to our original hypotheses and previous animal studies, axial diffusivity did not discriminate among categories of axonal injury within MS subjects. Animal models with axonal damage have demonstrated decreased $\lambda_{||}$ in the acute setting, but DTI studies of animal models with long-standing disease have not yet been reported. A potential explanation for the lack of correlation is that following significant axonal drop-out, the diffusivity of the remaining axons is overshadowed by the increased diffusivity due to gliosis and increased extracellular space. $\lambda_{||}$ may undergo a dynamic change, decreasing in the acute axonal damage setting and eventually increasing to values much greater than normal. This is supported by *in vivo* data in acute versus chronic optic neuritis (Naismith et al., 2009). Naismith et al. demonstrated in optic neuritis that $\lambda_{||}$ was decreased in the acute setting but was increased compared to normal controls at 1 year in the same subjects. Therefore, the lack of correlation between axial diffusivity and axonal loss in the present study may reflect the timing of the DTI studies relative to lesion onset, and may not be inconsistent with its ability to detect acute axonal loss that has been appreciated in animal studies. There is additional evidence from this study that in the setting of chronic MS, where $\lambda_{||}$ and $\lambda_{\perp}$ may be increased in a similar proportion, anisotropy may remain relatively unchanged and therefore less informative. This is in contrast to other settings where a differential increase in $\lambda_{\perp}$ or decrease in $\lambda_{||}$ may result in decreased anisotropy.

While this study examines DTI in *ex vivo* MS spinal cord, past studies have examined DTI in *ex vivo* MS brain. Schmierer et al. (2007) examined DTI in postmortem brain samples and found that ADC and fractional anisotropy (FA) were primarily affected by myelin content and to a lesser extent axonal loss and gliosis. Directional diffusivities were not evaluated in their postmortem brain study. Additionally, fixation presents a potential confounder in DTI histopathology correlation studies. The effect of fixation on DTI was previously explored. In both animal and human postmortem studies pre- and post-fixation, fixed tissue decreases water diffusivity while leaving diffusion anisotropy largely preserved (Schmierer et al., 2008; Sun et al., 2003). Fixation in mouse brain led to a two- to three-fold decrease in mean diffusivity while $\lambda_{||}$ and $\lambda_{\perp}$, when normalized to mean diffusivity, remained unchanged (Sun et al., 2003). Relative anisotropy was also unchanged following fixation. In human brain, $\lambda_{||}$, $\lambda_{\perp}$ and mean diffusivity were decreased in unfixed *ex vivo* brain compared to *in vivo* conditions and dropped further following fixation while FA remained unchanged (Schmierer et al., 2007). In our study, time from expiration to beginning fixation did not correlate with any DTI parameter. However, the effect of fixation remains a potential confounding variable in *ex vivo* DTI studies.

This study adds to our understanding of the observation of diffuse changes in the brain and spinal cord in MS. When ROIs were selected in MS spinal cords that appeared normal or near normal by LFB staining (i.e. outside of distinct lesions), these areas still reflected diffusion parameters ($\lambda_{||}$, ADC and a trend for $\lambda_{\perp}$) that were increased compared to controls. This finding is in accord with other studies that have demonstrated abnormal DTI values in areas of NAWM or diffusely abnormal white matter (DAWM) (Seewann et al., 2009; Werring et al., 1999). These NAWM or DAWM areas in other studies are likely the equivalent of the ROIs in this study labeled the most histologically normal. This finding gives additional evidence for diffuse abnormalities in MS spinal cords following years of MS.

Recently, several *in vivo* DTI studies have been reported involving MS spinal cord, brain, and optic nerve. Benedetti et al. (2010) reported lower spinal cord FA in SPMS patients compared to benign MS patients. In another study in MS spinal cords without distinct lesions, spinal cord FA and the ratio $\lambda_{||}/\lambda_{\perp}$ demonstrated abnormalities compared to control spinal cords (van Hecke et al., 2009). Highly increased radial diffusivity has been associated with severe demyelination and axonal loss, correlating with the development of persistent T1 hypointensities or "black holes" in gadolinium enhancing brain lesions (Naismith et al., 2010b). Additionally, radial diffusivity has correlated strongly with visual outcomes in remote optic neuritis (Naismith et al., 2010).

The importance of postmortem studies such as the present study is that they allow for direct correlation of pathology and imaging for validation of *in vivo* studies. Multiple sclerosis includes several types of pathology (demyelination, inflammation, axon loss, gliosis) that do not always exist concurrently. A complication in examining *ex vivo* spinal cords includes the complex interplay of these pathologies that can be present in concert or independently to some extent (Bitsch et al., 2000; DeLuca et al., 2006). In our study, demyelination and axonal loss correlated with one another, but differences in diffusion parameters at high and low axonal counts did not vary differentially based on the level of demyelination. Additionally, gliosis was appreciated in the majority of spinal cords samples but was not formally quantified. The resultant changes in structural architecture may partially account for decreased anisotropy in samples with both severe demyelination and axonal loss.

Another limitation of postmortem studies on the pathologic correlates of MRI is that samples are biased towards long-standing progressive disease. In this study, subjects had secondary progressive disease with chronic spinal cord lesions that largely lacked active inflammation. This provides an additional challenge to translating postmortem studies such as ours to *in vivo* conditions where inflammation is frequently present. Thus, no conclusions about the effect of inflammation on diffusion parameters can be drawn. Autopsy studies may also be biased toward severe lesions. Although spinal cord involvement may correlate with level of physical disability, the low variance in disability within the group of nine MS subjects in this study did not allow for correlation. Nonetheless, DTI still holds promise as a candidate imaging biomarker for disability correlation *in vivo*.

Conclusion

This study demonstrates sensitivity of $\lambda_{\perp}$ for the degree of demyelination in spinal cord lesions, but with less specificity than previous animal studies. In contrast, $\lambda_{||}$ did not correlate well with axonal loss. Diffusion tensor imaging also demonstrated diffuse changes within the normal-appearing spinal cord of MS patients *ex vivo*. This study provides a foundation for further exploration of DTI as a disease marker in MS.

Disclosures

The study is sponsored by grants from the National Institutes of Health (R01 NS054194) and the National MS Society (CA1012, RG

3670A3/2). The sponsors had no role in the study design, in the collection, analysis and interpretation of data, in the writing of the report, or in the decision to submit the paper for publication.

Dr. Klawiter has received speaking honoraria from Bayer Healthcare and Teva Neuroscience.

Dr. Schmidt has nothing to disclose.

Dr. Trinkaus has nothing to disclose.

Ms. Liang has nothing to disclose.

Dr. Budde has nothing to disclose.

Dr. Naismith has received consulting fees and/or speaking honoraria from Acorda Therapeutics, Bayer Healthcare, Biogen-Idec, EMD Serono, Teva Neuroscience, and Questcor.

Dr. Song has nothing to disclose.

Dr. Cross has received consulting fees or speaking honoraria from Teva Neuroscience, Biogen-Idec, Genentech Inc., Bayer Healthcare, BioMS, Eli Lilly, Sanofi-Aventis and Hoffman-La Roche.

Dr. Benzinger has received research grants or consulting fees from Renovo, Avid, Biomedical Systems, and ICON Medical Imaging.

Acknowledgments

NIH funding included R01 NS054194 (S.K.S.), P01 NS059560 (A.H.C.), R01 DK19645 (R.E.S.), K23NS052430-01A1 (R.T.N.) and UL1RR024992 (E.C.K.). National MS Society funding included CA1012 (A.H.C.) and RG 3670A3/2 (S.K.S.). E.C.K. was supported by an American Academy of Neurology Foundation Clinical Research Training Fellowship. A.H.C. was supported in part by the Manny and Rosalyn Rosenthal-Dr. John L. Trotter Chair in Neuroimmunology of Barnes-Jewish Hospital Foundation. T.B. was supported by a Bracco/American Roentgen Ray Society Scholar Award.

References

Agosta, F., Absinta, M., Sormani, M.P., Ghezzi, A., Bertolotto, A., Montanari, E., Comi, G., Filippi, M., 2007. In vivo assessment of cervical cord damage in MS patients: a longitudinal diffusion tensor MRI study. Brain 130, 2211–2219.

Barkhof, F., 1999. MRI in multiple sclerosis: correlation with expanded disability status scale (EDSS). Mult. Scler. 5, 283–286.

Barnes, D., Munro, P.M., Youl, B.D., Prineas, J.W., McDonald, W.I., 1991. The longstanding MS lesion. A quantitative MRI and electron microscopic study. Brain 114 (Pt 3), 1271–1280.

Basser, P.J., Pierpaoli, C., 1998. A simplified method of measuring the diffusion tensor using seven MR images. Magn. Reson. Med. 39, 928–934.

Benedetti, B., Rocca, M.A., Rovaris, M., Caputo, D., Zaffaroni, M., Capra, R., Bertolotto, A., Martinelli, V., Comi, G., Filippi, M., 2010. A diffusion tensor MRI study of cervical cord damage in benign and secondary progressive multiple sclerosis patients. J. Neurol. Neurosurg. Psychiatry 81, 26–30.

Bergers, E., Bot, J.C., De Groot, C.J., Polman, C.H., Lycklama a Nijeholt, G.J., Castelijns, J.A., van der Valk, P., Barkhof, F., 2002. Axonal damage in the spinal cord of MS patients occurs largely independent of T2 MRI lesions. Neurology 59, 1766–1771.

Bitsch, A., Schuchardt, J., Bunkowski, S., Kuhlmann, T., Bruck, W., 2000. Acute axonal injury in multiple sclerosis: correlation with demyelination and inflammation. Brain 123, 1174–1183. doi:10.1093/brain/123.6.1174.

Bookstein, F., 1989. Principal warps: thin-plate splines and the decomposition of deformations. IEEE Trans. Pattern Anal. Mach. Intell. 11, 567–585.

Bot, J.C., Barkhof, F., Polman, C.H., Lycklama a Nijeholt, G.J., de Groot, V., Bergers, E., Ader, H.J., Castelijns, J.A., 2004a. Spinal cord abnormalities in recently diagnosed MS patients: added value of spinal MRI examination. Neurology 62, 226–233.

Bot, J.C., Blezer, E.L., Kamphorst, W., Lycklama, A.N.G.J., Ader, H.J., Castelijns, J.A., Ig, K.N., Bergers, E., Ravid, R., Polman, C., Barkhof, F., 2004b. The spinal cord in multiple sclerosis: relationship of high-spatial-resolution quantitative MR imaging findings to histopathologic results. Radiology 233, 531–540.

Brex, P.A., Ciccarelli, O., O'Riordan, J.I., Sailer, M., Thompson, A.J., Miller, D.H., 2002. A longitudinal study of abnormalities on MRI and disability from multiple sclerosis. N. Engl. J. Med. 346, 158–164.

Budde, M.D., Kim, J.H., Liang, H.F., Schmidt, R.E., Russell, J.H., Cross, A.H., Song, S.K., 2007. Toward accurate diagnosis of white matter pathology using diffusion tensor imaging. Magn. Reson. Med. 57, 688–695.

Budde, M.D., Xie, M., Cross, A.H., Song, S.K., 2009. Axial diffusivity is the primary correlate of axonal injury in the experimental autoimmune encephalomyelitis spinal cord: a quantitative pixelwise analysis. J. Neurosci. 29, 2805–2813.

Cook, L.L., Foster, P.J., Mitchell, J.R., Karlik, S.J., 2004. In vivo 4.0-T magnetic resonance investigation of spinal cord inflammation, demyelination, and axonal damage in chronic-progressive experimental allergic encephalomyelitis. J. Magn. Reson. Imaging 20, 563–571.

DeBoy, C.A., Zhang, J., Dike, S., Shats, I., Jones, M., Reich, D.S., Mori, S., Nguyen, T., Rothstein, B., Miller, R.H., Griffin, J.T., Kerr, D.A., Calabresi, P.A., 2007. High resolution diffusion tensor imaging of axonal damage in focal inflammatory and demyelinating lesions in rat spinal cord. Brain 130, 2199–2210.

DeLuca, G.C., Williams, K., Evangelou, N., Ebers, G.C., Esiri, M.M., 2006. The contribution of demyelination to axonal loss in multiple sclerosis. Brain 129, 1507–1516.

Ferguson, B., Matyszak, M.K., Esiri, M.M., Perry, V.H., 1997. Axonal damage in acute multiple sclerosis lesions. Brain 120 (Pt 3), 393–399.

Filippi, M., Cercignani, M., Inglese, M., Horsfield, M.A., Comi, G., 2001. Diffusion tensor magnetic resonance imaging in multiple sclerosis. Neurology 56, 304–311.

Ghosh, N., DeLuca, G.C., Esiri, M.M., 2004. Evidence of axonal damage in human acute demyelinating diseases. J. Neurol. Sci. 222, 29–34.

Naismith, R.T., Xu, J., Tutlam, N.T., Scully, P.T., Trinkaus, K., Cross, A.H., Song, S.K., 2010a. Radial diffusivity in remote optic neuritis discriminates visual outcomes. Neurology 74, 1702–1707.

Naismith, R.T., Xu, J., Tutlam, N.T., Scully, P.T., Trinkaus, K., Snyder, A.Z., Song, S.K., Cross, A.H., 2010b. Increased diffusivity in acute multiple sclerosis lesions predicts risk of black hole. Neurology 74, 1694–1701.

Naismith, R.T., Xu, J., Tutlam, N.T., Scully, P.T., Trinkaus, K., Snyder, A.Z., Song, S.K., Cross, A.H., 2010c. Increased diffusivity in acute multiple sclerosis lesions predicts risk of black hole. Neurology 74, 1694–1701.

Naismith, R.T., Xu, J., Tutlam, N.T., Snyder, A., Benzinger, T., Shimony, J., Shepherd, J., Trinkaus, K., Cross, A.H., Song, S.K., 2009. Disability in optic neuritis correlates with diffusion tensor-derived directional diffusivities. Neurology 72, 589–594.

Naismith, R.T., Xu, J., Tutlam, N.T., Trinkaus, K., Cross, A.H., Song, S.K., 2010. Radial diffusivity in remote optic neuritis discriminates visual outcomes. Neurology 74, 1702-1710.

Nijeholt, G.J., van Walderveen, M.A., Castelijns, J.A., van Waesberghe, J.H., Polman, C., Scheltens, P., Rosier, P.F., Jongen, P.J., Barkhof, F., 1998. Brain and spinal cord abnormalities in multiple sclerosis. Correlation between MRI parameters, clinical subtypes and symptoms. Brain 121 (Pt 4), 687–697.

Noseworthy, J.H., Lucchinetti, C., Rodriguez, M., Weinshenker, B.G., 2000. Multiple sclerosis. N. Engl. J. Med. 343, 938–952.

Schmierer, K., Wheeler-Kingshott, C.A., Boulby, P.A., Scaravilli, F., Altmann, D.R., Barker, G.J., Tofts, P.S., Miller, D.H., 2007. Diffusion tensor imaging of post mortem multiple sclerosis brain. Neuroimage 35, 467–477.

Schmierer, K., Wheeler-Kingshott, C.A., Tozer, D.J., Boulby, P.A., Parkes, H.G., Yousry, T.A., Scaravilli, F., Barker, G.J., Tofts, P.S., Miller, D.H., 2008. Quantitative magnetic resonance of postmortem multiple sclerosis brain before and after fixation. Magn. Reson. Med. 59, 268–277.

Seewann, A., Vrenken, H., van der Valk, P., Blezer, E.L., Knol, D.L., Castelijns, J.A., Polman, C.H., Pouwels, P.J., Barkhof, F., Geurts, J.J., 2009. Diffusely abnormal white matter in chronic multiple sclerosis: imaging and histopathologic analysis. Arch. Neurol. 66, 601–609.

Song, S.K., Sun, S.W., Ju, W.K., Lin, S.J., Cross, A.H., Neufeld, A.H., 2003. Diffusion tensor imaging detects and differentiates axon and myelin degeneration in mouse optic nerve after retinal ischemia. Neuroimage 20, 1714–1722.

Song, S.K., Sun, S.W., Ramsbottom, M.J., Chang, C., Russell, J., Cross, A.H., 2002. Dysmyelination revealed through MRI as increased radial (but unchanged axial) diffusion of water. Neuroimage 17, 1429–1436.

Song, S.K., Yoshino, J., Le, T.Q., Lin, S.J., Sun, S.W., Cross, A.H., Armstrong, R.C., 2005. Demyelination increases radial diffusivity in corpus callosum of mouse brain. Neuroimage 26, 132–140.

Stankiewicz, J.M., Neema, M., Alsop, D.C., Healy, B.C., Arora, A., Buckle, G.J., Chitnis, T., Guttmann, C.R., Hackney, D., Bakshi, R., 2009. Spinal cord lesions and clinical status in multiple sclerosis: a 1.5 T and 3 T MRI study. J. Neurol. Sci. 279, 99–105.

Sun, S.W., Neil, J.J., Song, S.K., 2003. Relative indices of water diffusion anisotropy are equivalent in live and formalin-fixed mouse brains. Magn. Reson. Med. 50, 743–748.

Tallantyre, E.C., Bo, L., Al-Rawashdeh, O., Owens, T., Polman, C.H., Lowe, J., Evangelou, N., 2009. Greater loss of axons in primary progressive multiple sclerosis plaques compared to secondary progressive disease. Brain 132, 1190–1199.

Trapp, B.D., Peterson, J., Ransohoff, R.M., Rudick, R., Mork, S., Bo, L., 1998. Axonal transection in the lesions of multiple sclerosis. N. Engl. J. Med. 338, 278–285.

van Hecke, W., Nagels, G., Emonds, G., Leemans, A., Sijbers, J., van Goethem, J., Parizel, P.M., 2009. A diffusion tensor imaging group study of the spinal cord in multiple sclerosis patients with and without T2 spinal cord lesions. J. Magn. Reson. Imaging 30, 25–34.

Werring, D.J., Clark, C.A., Barker, G.J., Thompson, A.J., Miller, D.H., 1999. Diffusion tensor imaging of lesions and normal-appearing white matter in multiple sclerosis. Neurology 52, 1626–1632.